Journal of Structural Geology, Vol. 13, No. 2, pp. 123 to 136, 1991
Printed in Great Britain

0191-8141/91 $03.00 + 0.00
Pergamon Press plc

Historical surface faulting in the Basin and Range province, western North America: implications for fault segmentation

CRAIG M. DEPOLO

Nevada Bureau of Mines and Geology, Mackay School of Mines, University of Nevada, Reno, NV 89557, U.S.A.

DOUGLAS G. CLARK and D. BURTON SLEMMONS

Center for Neotectonic Studies, Mackay School of Mines, University of Nevada, Reno, NV 89557, U.S.A.

and

ALAN R. RAMELLI

Nevada Bureau of Mines and Geology, Mackay School of Mines, University of Nevada, Reno, NV 89557, U.S.A.

(*Received* 21 *December* 1989; *accepted in revised form* 20 *June* 1990)

Abstract—The distribution of surface ruptures caused by 11 historical earthquakes in the Basin and Range province of western North America provides a basis for evaluating earthquake segmentation behavior of faults in extensional tectonic settings. Two of the three moderate magnitude ($5.5 < M < 7$) events appear to be confined to individual geometric or structural segments. The remaining nine events, eight of which had large magnitudes ($M \geq 7$), ruptured multiple geometric or structural segments. Several of these events had widely distributed surface-rupture patterns, ruptured in complex manners, and extended beyond distinct fault-zone discontinuities. Some of the surface ruptures associated with these events may have resulted from sympathetic or secondary surface faulting. Approximately one-half of the surface rupture end points coincided with distinct fault-zone discontinuities.

This study indicates that earthquake ruptures in extensional tectonic settings may not be confined to individual geometric or structural segments. Some rupture-controlling discontinuities may be difficult to identify and significant faulting may occur beyond postulated rupture end points. Rupture of multiple geometric or structural segments should be considered in the evaluation of large earthquakes. Several lines of evidence, particularly timing information, are needed to delineate potential earthquake segments in the Basin and Range province.

INTRODUCTION

INDIVIDUAL historical earthquakes rarely rupture entire fault zones (Albee & Smith 1966). Seismic hazard analyses, therefore, require an estimate of how much of a given fault zone will rupture during future earthquakes to characterize earthquake sizes. Several techniques have been developed to estimate potential earthquake-rupture lengths, including half-length, fractional fault length and fault segmentation techniques (dePolo & Slemmons in press). Of these, the fault segmentation technique is the most appealing, principally because it incorporates more physical and paleoseismic information than other techniques. Fault segmentation modeling involves the division of fault zones into discrete segments separated by rupture-controlling discontinuities.

This paper summarizes 11 historical earthquakes from the Basin and Range extensional province (Fig. 1). These events exhibit a wide range of variability in their surface rupture patterns, from simple to very complex. The goal of this study was to explore the features that may have controlled or influenced the ends of these earthquake ruptures and to characterize the ruptures with respect to fault segments. Surface ruptures with normal, normal-oblique and strike-slip senses of displacement are represented.

Three types of surface rupture are considered in this paper: primary, secondary and sympathetic. Primary surface rupture is fault displacement that is believed to be directly connected to subsurface seismogenic displacement, whereas secondary surface rupture has a branching or secondary relation to the main seismogenic fault. Sympathetic surface rupture is triggered slip along a fault that is 'isolated' from the main seismogenic fault.

FAULT SEGMENTATION

Fault segmentation has been described at a wide range of scales and with varying criteria. This has led to different definitions of the term "segment", making it important to understand a specific author's definition of the word and to clearly define the term when using it. This study examines historical "earthquake segments", or those parts of a fault zone or fault zones that have

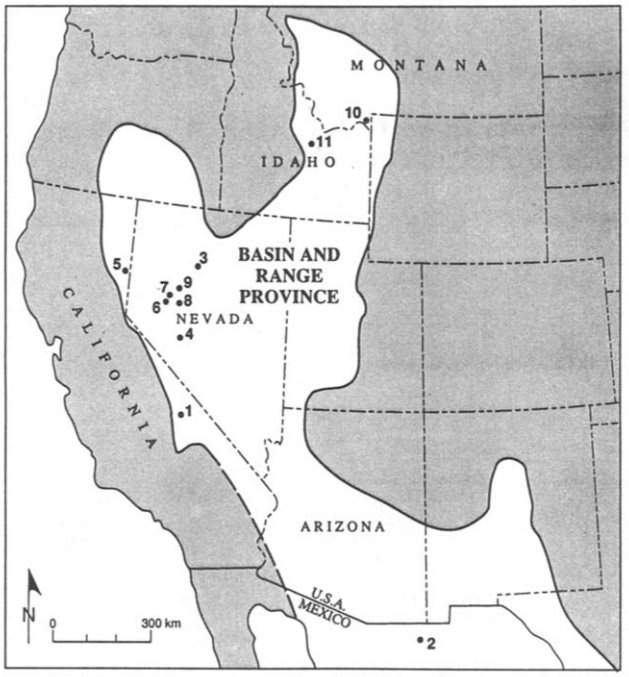

Fig. 1. Location map of primary surface faulting earthquakes in the Basin and Range province, western North America. **1**, 1872 Owens Valley; **2**, 1887 Sonora, Mexico; **3**, 1915 Pleasant Valley; **4**, 1932 Cedar Mountain; **5**, 1950 Fort Sage Mountain; **6**, 1954 Rainbow Mountain; **7**, 1954 Stillwater; **8**, 1954 Fairview Peak; **9**, 1954 Dixie Valley; **10**, 1959 Hebgen Lake; **11**, 1983 Borah Peak. Boundary of the Basin and Range province modified from Stewart (1983).

ruptured during individual earthquakes. Large earthquake segments may comprise one or more fault segments as defined in other ways, such as by fault geometry or fault structure (geometric and structural segments, respectively).

Earthquake segmentation involves the identification and characterization of discontinuities along fault zones which may potentially act as barriers to earthquake ruptures. Many compilations of the characteristics of fault-zone discontinuities have been presented (e.g. Schwartz & Coppersmith 1984, 1986, Slemmons & dePolo 1986, Knuepfer *et al.* 1987, Barka & Kadinsky-Cade 1988, Wheeler & Krystinik 1988, dePolo *et al.* 1989, Knuepfer 1989, Crone & Haller 1991). Indicators of fault-zone discontinuities include: geometric, structural, behavioral, paleoseismic, geomorphic, geological, geophysical and rheological data (dePolo *et al.* 1989). Several lines of evidence are needed to identify a potential earthquake discontinuity and to evaluate its persistence through time. An important consideration for earthquake discontinuities is scale; in general, only the larger features (scales on the order of hundreds of meters to kilometers) appear capable of arresting propagating earthquake ruptures (Sibson 1989, Crone & Haller 1991).

The most common fault-zone discontinuities can be grouped into three major categories: geometric, structural and behavioral. These distinctions are used for descriptive purposes; there are 'gray areas' between categories and some discontinuities may fit into more than one category. Geometric discontinuities include changes in fault orientation (bends), step overs, and separations or gaps in a fault zone (see Crone & Haller 1991). Wheeler (1987) pointed out that geometric discontinuities in plan view may not have a significant effect on earthquake ruptures with a normal sense of displacement. An abrupt bend in plan view of a normal fault, for example, can accommodate a vertical-slip vector, and would not necessarily inhibit a propagating rupture. Thus, the sense of displacement is an important factor to consider in the evaluation of geometric data. Structural discontinuities include fault branches, intersections with other faults and folds, and terminations at cross structures. Since the ends of fault zones can be considered structural discontinuities, distinct or individual faults can be classified as structural segments. Behavioral discontinuities include changes in slip rates, interseismic intervals, senses of displacement or creeping vs locked behavior.

Paleoseismic data can clarify the rupture histories of earthquake segments and the long-term behavior of discontinuities. In this paper, paleoseismicity refers specifically to prehistoric earthquakes. Determining the history and lateral extent of paleoearthquake segments along a fault zone can provide direct temporal and spatial evidence of previous segmented behavior. Unfortunately, paleoseismic data are limited for most of the events presented in this paper.

BASIN AND RANGE PROVINCE

The Basin and Range province of the western United States and northern Mexico is an actively deforming Cenozoic extensional province (Fig. 1). Spatial and temporal variations in the rates of activity and in the style of faulting have occurred within this province throughout the Cenozoic. Contemporary rates of tectonic activity are higher in the northern part of the province and along its eastern and western margins. Regions of active extension are marked by high heat flow, thin crust, sparsely distributed bimodal volcanism and earthquakes with focal depths generally limited to 10–15 km or less. Geologic, geomorphic and geophysical data indicate that extensional tectonism has resulted in widespread domains of tilted fault blocks, horst and graben development, and a heterogeneous upper crust, both structurally and lithologically (Stewart 1980). Historical seismicity in the province is concentrated in three major belts: (1) the western margin of the province, (2) the central Nevada–eastern California seismic belt, within the western part of the province; and (3) the northern part of the Intermountain seismic belt, along the eastern margin of the province.

HISTORICAL SURFACE-FAULTING EVENTS

Eleven earthquakes that have been associated with primary tectonic surface rupture in the Basin and Range

Table 1. Historical primary, tectonic surface faulting events in the Basin and Range province. Number corresponds to those in Fig. 1. M = moment or intensity magnitude, undifferentiated, M_w = moment magnitude, M_s = surface-wave magnitude, M_L = local magnitude

No.	Date	Magnitude	Earthquake or fault	Main style of surface faulting
1	26 March 1872	M = 7.7–8.0+	Owens Valley, California	Strike-slip
2	03 May 1887	M_w = 7.2–7.4	Sonora, Mexico	Normal
3	03 October 1915	M_s = 7.6	Pleasant Valley, Nevada	Normal
4	21 December 1932	M_s = 7.2	Cedar Mtn, Nevada	Strike-slip
5	14 December 1950	M_L = 5.6	Fort Sage Mtn, California	Normal
6	06 July 1954	M_s = 6.3	Rainbow Mtn, Nevada	Normal
7	24 August 1954	M_s = 7	Stillwater, Nevada	Normal
8	16 December 1954	M_s = 7.2	Fairview Peak, Nevada	Normal-oblique
9	16 December 1954	M_s = 6.8	Dixie Valley, Nevada	Normal
10	17 August 1959	M_s = 7.5	Hebgen Lake, Montana	Normal
11	29 October 1983	M_s = 7.3	Borah Peak, Idaho	Normal

province are reviewed in this paper (Table 1 and Fig. 1). These events are not uniformly distributed throughout the Basin and Range province, but occur in discrete spatial and temporal groupings (Wallace 1987). Seven of the 11 events occurred in the NNE-trending central Nevada–eastern California seismic belt (Wallace 1984a); the 1959 Hebgen Lake and 1983 Borah Peak earthquakes are located in the Intermountain seismic belt.

Due to variations in the types of magnitude reported for different events, different magnitude scales are used here. These events, however, lie within a magnitude range over which these different scales are reasonably comparable (see Kanamori 1983). The following acronyms are used in this paper to distinguish the different scales: (M_s) surface-wave magnitude, (M_L) local magnitude, (M_w) moment magnitude and (M) undifferentiated moment or intensity magnitudes.

1872 *Owens Valley, California, earthquake*

The 26 March 1872 Owens Valley earthquake is the largest historical event in the Basin and Range province, in terms of estimated magnitude, maximum displacement and rupture length. It had an estimated magnitude of M7.7–8+, and was felt strongly over an area of 324,000 km^2 (Oakeshott *et al.* 1972, Coffman & von Hake 1973, Hanks & Kanamori 1979, Beanland & Clark in press). The earthquake caused about 90–110 km of surface faulting along the Owens Valley fault zone (OVFZ) (Fig. 2). Surface displacements were dominantly right-lateral strike-slip, with a single-trace maximum lateral offset of 7 m, an average lateral offset of 6 m, a maximum vertical offset of 4.4 m and an average vertical offset of 1 m (Beanland & Clark in press). A maximum surface displacement of 11 m (normal-right oblique) is derived by adding displacement from two parallel fault traces in the Lone Pine area (Lubetkin & Clark 1988, Beanland & Clark in press). The surface rupture consisted of a relatively straight central section located in the middle of a large graben (Owens Valley) and more distributed, non-linear northern and southern sections (Fig. 2).

The north and south ends of the 1872 rupture are at or near extensional basins. The north end of the rupture zone steps and distributes slip into the northern Owens Valley, creating small closed depressions (Fig. 2, point A). The exact position of the southern end of the 1872 surface rupture is less certain. The 1872 rupture clearly

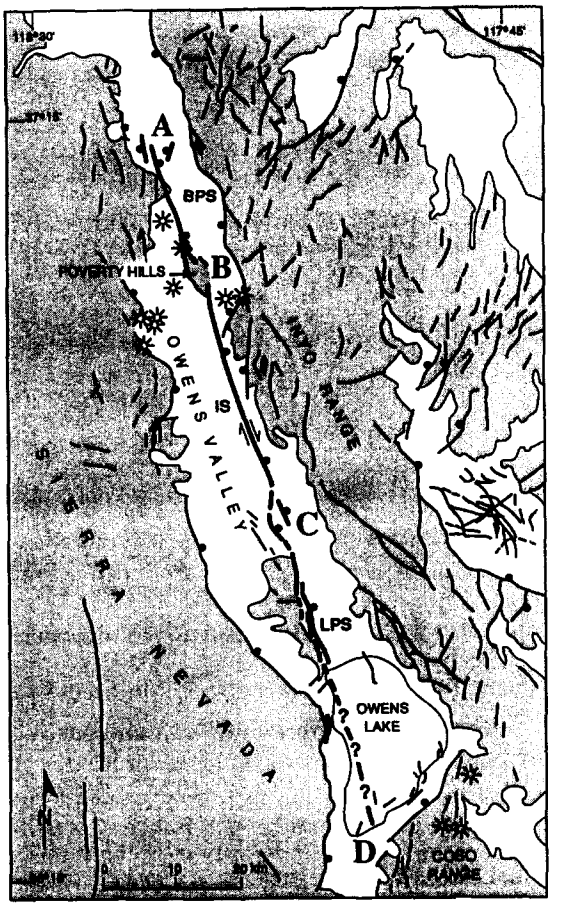

Fig. 2. Surface ruptures from the 1872 Owens Valley earthquake (from Beanland & Clark in press). BPS = Big Pine segment, IS = Independence segment, LPS = Lone Pine segment. Stars are Quaternary volcanic centers. Bedrock from Matthews & Burnett (1965), Strand (1967), Streitz & Stinson (1974) and Dunne *et al.* (1978). Bold lines denote the surface ruptures. Medium weight lines denote other selected faults. Balls are shown on the downthrown side of faults with normal components. Thrust faults are shown with barbs. Patterned areas are bedrock. White areas are alluviated valleys and basins. The large letters on figures are end points or discontinuities discussed in text.

offsets shorelines at the northern edge of Owens Lake, whereas near the southern edge, the amount of tectonic displacement is less clear due to extensive liquefaction. The southern end of the 1872 rupture is probably terminated where the southern Owens Lake basin is bounded by NE-trending faults and the Coso Range (Fig. 2, point D).

Beanland & Clark (in press) divide the OVFZ into seven segments on the basis of fault continuity, strike and style. We apply a more generalized segmentation criteria than Beanland & Clark, although we adopt some of their segment names. From south to north, the OVFZ can be divided into at least three geometric segments (Fig. 2): the Lone Pine segment, the Independence segment and the Big Pine segment. These segments are defined primarily on the basis of geometric discontinuties. The exact location of the southern end of the Lone Pine segment is uncertain, but it appears to terminate near intersecting cross faults (Fig. 2, point D). Because of the presence of young lacustrine sediments and liquefaction features, the OVFZ is difficult to delineate along the southern 18 km of this segment. Based on a 1-km-wide right step and a slightly more westerly strike of lineaments and faults mapped by Carver (1969) in the dried Owens Lake bottom, the distinction of this southern part as a fourth geometric segment may be warranted. The Lone Pine segment is distinct from near the northern part of Owens Lake northward for about 32 km to a 1.5-km-wide right step (approximate cross-strike distance) between the Lone Pine and Independence segments (Fig. 2, point C). The Lone Pine segment is as much as 2.5 km wide, and has a greater surface trace complexity and a larger normal component than the Independence segment. The Independence segment (35 km long) is a remarkably linear, narrow fault zone (as much as 0.5 km wide), with small sag ponds and other minor structural complexities, such as small steps in the fault trace. At the northern end of the Independence segment, the Poverty Hills form a prominent discontinuity in the OVFZ (Fig. 2, point B). The presence of this discontinuity is interpreted based on several factors: (1) change in fault geometry and distribution; (2) intersections with other faults; (3) a postulated left step in the fault zone (Martel 1984); (4) a bedrock high between the Owens Lake and Bishop basins and associated geophysical anomalies; and (5) Quaternary volcanism. The 1872 surface rupture was deflected across Poverty Hills, but the discontinuity did not terminate the rupture. The Big Pine segment extends for 23 km northward from the Poverty Hills. This segment trends slightly more westerly than the rest of the OVFZ and exhibits a complex pattern with several fault strands.

The 1872 event is interpreted to have ruptured at least three geometric segments along the OVFZ. Differences in surface complexity and in the amount of vertical slip component between the Lone Pine and Independence segments further distinguishes these as behavioral segments. The OVFZ shows evidence of at least two prior Holocene events which may have ruptured the same segments as in 1872 (Beanland & Clark 1987).

1887 *Sonora, Mexico, earthquake*

The 3 May 1887 Sonora earthquake, in the southern Basin and Range province, had an estimated magnitude of $\mathbf{M}_w$7.2–7.4 and an estimated felt area of nearly 2,000,000 km^2 (Dubois & Smith 1980, Dubois & Sbar 1981, Herd & McMasters 1982). Dominantly normal-slip surface faulting occurred along approximately 75 km of the Pitaycachi fault (Bull & Pearthree 1988), making this the longest normal-slip surface rupture in the worldwide historical record. Fault scarps produced during this event ranged in height from 0.5 to 4+ m (Bull & Pearthree 1988, Pearthree *et al.* 1990). Herd & McMasters (1982) measured a maximum normal-slip displacement of 5.1 m.

Surface faulting during the 1887 earthquake occurred along a mountain front–alluvium contact for much of the rupture length (Goodfellow 1888, Bull & Pearthree 1988). The surface rupture can be divided into three geometric segments (P. A. Pearthree personal communication 1988). The southern segment is about 22 km long and had less than 1 m vertical displacement, significantly less displacement than that to the north. It dies out in bedrock at its southern end, and is separated from the main rupture by a 2.5-km-wide right step (Fig. 3, points D and C). The central segment follows the mountain front of the Sierra de San Luis for much of its overall length of 39 km and includes the largest surface displacements. Near its southern end, the central segment departs from a 60° bend in the range front, has a right step of about 0.5 km, and extends 10 km to the south across a large valley, where it dies out just south of a bedrock hill within the valley. The northern 14 km of the surface rupture splays from the range front, follows an alluvium–pediment contact for several kilometers, and extends 5 km into the San Bernardino Valley (Bull & Pearthree 1988). This northern part of the rupture is considered a third segment based on a bend of approximately 30°, bifurcation into several parallel fault traces, and divergence from the range front (Fig. 3, point B). Surface ruptures and cumulative displacement are essentially continuous through this discontinuity.

The Sonora earthquake was associated with a relatively simple, narrow surface rupture, mainly along a range front. The surface rupture can be divided into three geometric segments. Bull & Pearthree (1988) estimated that about 200,000 years had elapsed since the event prior to 1887, and that the prehistoric surface rupture appears to be similar in length and amount of displacement to the historical earthquake.

1915 *Pleasant Valley, Nevada, earthquake*

The 3 October 1915 Pleasant Valley earthquake had a magnitude of $\mathbf{M}_s$7.6 (Bonilla *et al.* 1984), and was felt from southern Washington to northern Mexico, and from western Colorado to the Pacific coast. Four major fault scarps formed a right-stepping en échelon pattern (Fig. 4) for a combined, end-to-end rupture length of 60 km (Wallace 1984b). From northeast to southwest,

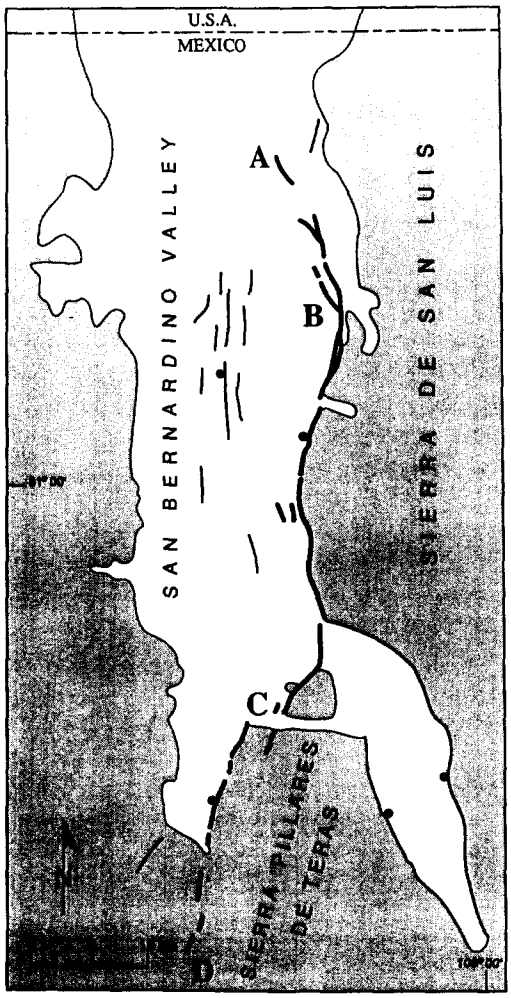

Fig. 3. Surface ruptures from the 1887 Sonora, Mexico, earthquake (from Bull & Pearthree 1988). Bedrock from Direccion General de Geografia del Territorio Nacional (1981) and Sumner (1977). Annotation as Fig. 2.

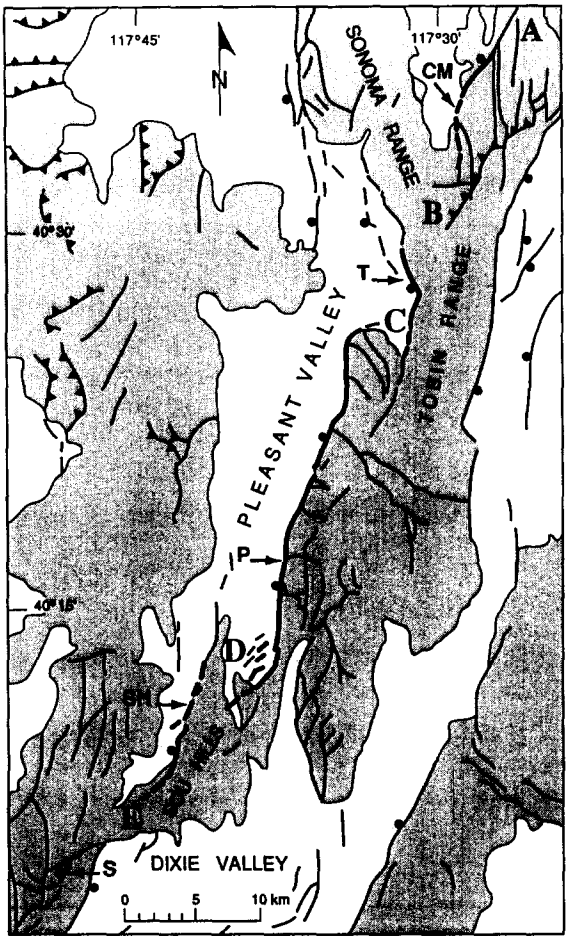

Fig. 4. Surface ruptures from the 1915 Pleasant Valley earthquake (from Wallace 1984b). CM = China Mountain segment, T = Tobin segment, P = Pearce segment, SH = Sou Hills segment, S = Stillwater segment. Bedrock from Stewart & Carlson (1978) and Wallace (1984a). Annotation as Fig. 2.

the major 1915 earthquake scarps are: China Mountain (length (L) = 10 km; maximum displacement (D_{max}) = 1.5 m), Tobin (L = 8.5 km; D_{max} = 4.7 m), Pearce (L = 30 km; D_{max} = 5.8 m) and Sou Hills (L = 10.5 km; D_{max} = 2.7 m). The cross-strike distances between the en échelon steps range from 3.5 to 6 km. A fifth scarp near the crest of the Stillwater Range (L = 1.5 km; D_{max} = 1.2? m) has been attributed to gravitational spreading (Wallace 1984b), but its position as a potential fifth right-step within a zone of faulting with a similar spacing, orientation and west-side-down character is consistent with a tectonic origin. If this scarp is tectonic, the total rupture-zone length is 74 km, and the southern step and gap in faulting is 10.4 km (Fig. 4, point E).

The four principal surface ruptures from the 1915 earthquake occurred near the base of W-facing range blocks and mainly followed pre-existing late Quaternary fault scarps. Faulting was predominately dip-slip, with a maximum vertical displacement of 5.8 m on the Pearce scarp, and an overall average vertical displacement of 2 m (Wallace 1984b). Up to 2 m of right-lateral offset occurred locally.

Surface rupture produced by the 1915 earthquake occurred along four or five structural or geometric segments, based on the continuity of horst blocks, the pattern of late Quaternary fault scarps, and large steps in the fault zone. The largest surface displacements were along the Pearce and Tobin segments (Page 1934). These two segments bound the west side of the Tobin Range and are separated by a 3.5-km-wide right step (Fig. 4, point C). This step distinguishes these as geometric segments. The China Mountain and Sou Hills ruptures bound different range blocks (separate from the Tobin Block), and are therefore considered structural segments.

The southern end of 1915 surface faulting (excluding the 1.5-km-long failure at the crest of the Stillwater Range) coincides with the Sou Hills transverse bedrock zone (Fonseca 1988) (Fig. 4, point E). Fonseca (1988) used geologic, geomorphic and paleoseismic data to show that the Sou Hills have acted as a profound barrier to propagating surface ruptures throughout the Quaternary. The southern end of surface faulting also coincides with aeromagnetic and gravity cross-structures, and a pronounced change in the tilt directions of range blocks north and south of the approximate latitude of

the Sou Hills (Stewart 1980, Thenhaus & Barnhard 1989).

The northern part of the 1915 surface rupture crossed the Tobin Range with a 6-km-wide step (cross-strike distance) in surface faulting between the Tobin and China Mountain scarps (Wallace 1984b) (Fig. 4, point B). The north end of the Tobin scarp is aligned with conspicuous late Quaternary fault scarps that continue tens of kilometers to the northwest along the west flank of the Tobin and Sonoma Ranges, which did not rupture in 1915 (Wallace 1984b).

The 1915 earthquake segment consisted of four and possibly five structural or geometric segments, which form an en échelon pattern with surface offsets separated by right steps as large as 6 km (cross-strike distances). Wallace (1989) suggested that the distributed surface-faulting pattern may be the result of displacement along a fault at depth that trends oblique to the surface faults, and only ruptured those portions of the surface faults located above the source zone.

1932 *Cedar Mountain, Nevada, earthquake*

The 21 December 1932 Cedar Mountain earthquake was a complex right-lateral strike-slip event that produced a widely distributed surface-rupture pattern (Gianessa & Callaghan 1934). This event had a magnitude of M_s7.2 and a felt area of 850,000 km^2 (Coffman & von Hake 1973, Abe 1981). The epicenter of the 1932 earthquake was located in or near Gabbs Valley, near the north end of the rupture zone (Gianella & Callaghan 1934) (Fig. 5). The zone of surface ruptures is approximately 60 km in length (end-to-end measurement), 6–14 km wide, and generally trends southeast from the epicentral area. Surface ruptures were not confined to a mountain front or a single topographic feature, but rather were distributed broadly across three valleys and short parts of adjacent mountain fronts. Parts of several faults were ruptured (Fig. 5), including the Stewart–Monte Cristo Valley fault zone (SMCFZ), and several shorter, unnamed faults in the Stewart and Gabbs Valleys (Molinari 1984a,b, dePolo *et al.* 1987b). Modeling of body waveforms from regional and teleseismic seismograms indicates that the main event consisted of two subevents that are spatially related to the northern and southern halves of the rupture zone (Doser 1988).

The northern termination of 1932 surface faulting is indistinct and consisted of several widely-spaced, small ruptures in Gabbs Valley that generally had displacements less than a few decimeters (Gianella & Callaghan 1934) (Fig. 5, point A). One of the northernmost ruptures occurred on the southern end of a fault that had small displacements during the 1954 Fairview Peak earthquake. The southern part of the 1932 rupture zone had longer and more narrowly confined surface breaks and larger displacements than the northern end, but also involved several, distributed fault traces. The longest and most continuous surface faulting occurred for about 17 km along the SMCFZ in northern Monte Cristo Valley, with maximum lateral displacements of 1–2 m

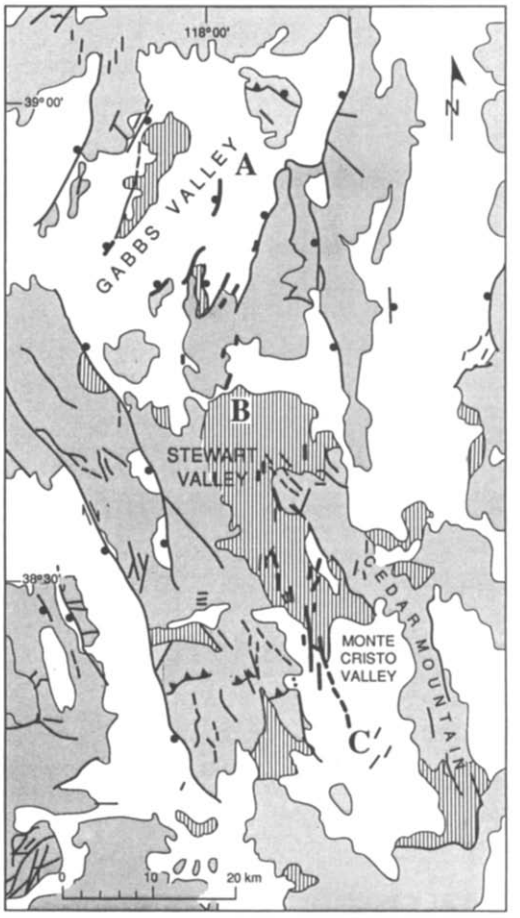

Fig. 5. Surface ruptures from the 1932 Cedar Mountain earthquake (from Gianella & Callaghan 1934, Molinari 1984a). Areas with vertical patterns are Tertiary sediments. Bedrock and Tertiary sediments from Stewart & Carlson (1978). Ruptures along the Stewart–Monte Cristo fault zone trend NNW from point C. Annotation as Fig. 2.

and normal-slip displacements of as much as 0.5 m (Molinari 1984a, dePolo *et al.* 1987a). The southern end of surface faulting is in the vicinity of cross-faults and an extensional basin (Fig. 5, point C).

The northern and southern areas of surface faulting (Fig. 5, point B) are separated by a 9-km gap in coseismic faulting. Within this gap in surface faulting, many folds are present in surficial and Miocene sedimentary deposits, but not in older volcanic and basement rocks (Molinari 1984a). Molinari (1984a) suggests that shallow detachment may be be responsible for these folds and that such deformation may account for the lack of discrete surface ruptures. Surface ruptures trend more northeasterly north of this gap in surface faulting than to the south.

The extent of surface rupture associated with the 1932 earthquake would have been difficult or impossible to predict due to the widespread distribution of many small surface ruptures. The distributed nature of surface faulting complicates application of fault segmentation modeling. The Cedar Mountain earthquake can be interpreted as being the result of multiple faults (structural segments) failing in sequence, potentially adding to the complexity of surface faulting and the event's magnitude.

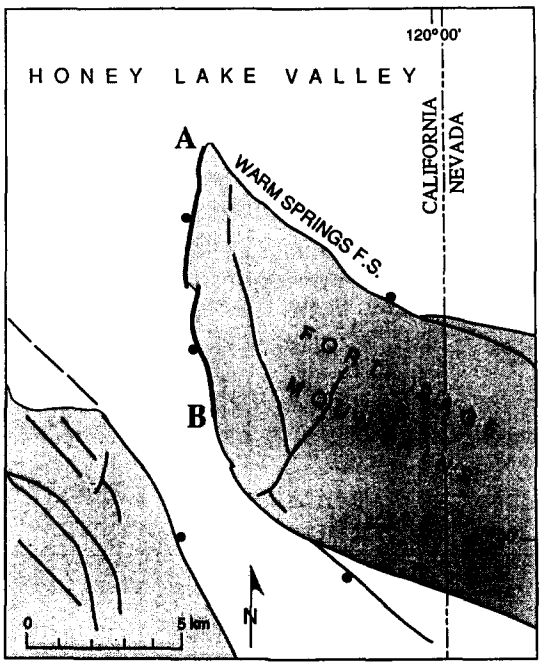

Fig. 6. Surface ruptures from the 1950 Fort Sage Mountain earthquake (from Gianella 1957). Bedrock from Lydon *et al.* (1960), Burnett & Jennings (1962) and Bonham (1969). Annotation as Fig. 2.

1950 *Fort Sage Mountains, California, earthquake*

The Fort Sage Mountains earthquake of 14 December 1950 had a magnitude of M_L5.6 and was felt over an area of 52,000 km^2 (Coffman & von Hake 1973, Bonilla *et al.* 1984). A 9.5-km-long scarp formed at the western base of the Fort Sage Mountains along the Fort Sage Mountains fault (Gianella 1951, 1957). The rupture was composed of two distinct, continuous breaks, separated by a 320-m left-step (Fig. 6). Although the maximum discrete offset at the surface was 20 cm, the surface displacement may have been as much as 60 cm if folding of alluvium is considered (Gianella 1957). The sense of displacement at the surface was normal slip with no evidence of lateral offset (Gianella 1957).

The Fort Sage Mountains, the Fort Sage Mountains fault, and the 1950 surface ruptures are ostensibly terminated at their northern end by the Warm Springs fault system (Fig. 6, point A), which bounds the northeastern side of the Fort Sage Mountains (Lydon *et al.* 1960, Bonham 1969, Grose 1984). The southern end of surface faulting is 2 km short of a 38° bend in the fault (Fig. 6, point B) and in the mountain front (broad salient). Surface ruptures from the 1950 earthquake appear to be confined to a single geometric segment.

1954 *Rainbow Mountain and Stillwater, Nevada, earthquakes*

The Rainbow Mountain and Stillwater earthquakes of 6 July and 24 August 1954 (M_S6.3 and 7, respectively) (Bonilla *et al.* 1984) were the first two of four closely spaced surface-rupturing earthquakes in west-central Nevada during a 6-month period.

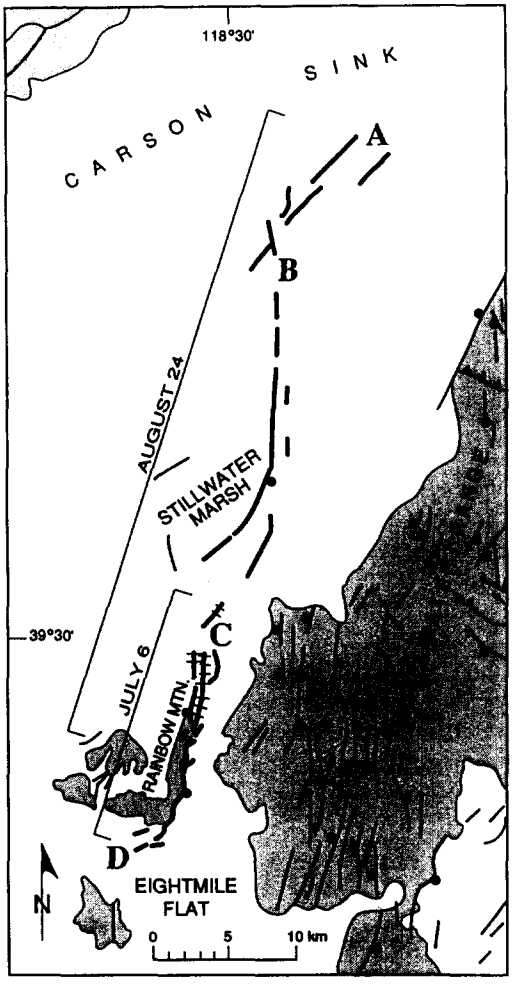

Fig. 7. Surface ruptures from the 1954 Rainbow Mountain and Stillwater earthquake (from Tocher 1956, Bell 1984). Hachured lines designate extent that ruptured during the 6 July and the 23 August earthquakes. The extent of surface rupturing from each of these earthquakes is shown in brackets. Bedrock from Morrison (1964) and Page (1965). Annotation as Fig. 2.

The 6 July event produced 18 km of surface faulting along a single structural segment (Fig. 7). Most of this rupture (~10 km) lies at the base of Rainbow Mountain. Extensive fractures and small E-facing scarps as much as 30 cm high formed along a NNW-trending zone along the eastern base of Rainbow Mountain and into adjacent Quaternary basins (Tocher 1956). Both ends of this rupture are somewhat diffuse, with surface ruptures distributing and dying out in young basin fill (Fig. 7, points C and D).

The 24 August Stillwater earthquake reactivated and increased the heights of fault scarps at the northern end of the 6 July rupture (Fig. 7) and also ruptured 34 km northward across the Stillwater Marsh to the Carson Sink (Tocher 1956, Bell 1984). The Stillwater earthquake produced scarps as much as 76 cm high. The location of the northern end of this rupture is somewhat uncertain, but surface faulting appears to die out near point A on Fig. 7. The southern end of surface faulting died out within the surface rupture produced by the Rainbow Mountain earthquake. Coseismic displacement from both events apparently occurred along at

least three fault traces (Fig. 7, hachured symbol). The August event is interpreted as consisting of two structural segments, based primarily on an intersecting relationship (Fig. 7, point B). A difference in strike of 40° also exists between these two segments.

Neither the July nor August earthquakes produced measureable lateral offsets at the surface (Tocher 1956). Focal mechanisms, however, indicate significant strike-slip components, particularly for the July event (Doser 1986). Doser (1986) modeled the July earthquake as a double event. The first subevent is believed to have produced the bulk of the seismic moment release and was dominated by strike-slip displacement, whereas the second subevent was shallower and had a larger normal-slip component. Doser suggested that the surface rupture may be more directly related to the second event, partially explaining the lack of lateral offset at the surface.

The July and August surface ruptures broke along faults that had little or no tectonic surface deformation since the deposition of ~12,000 year Lake Lahonton sediments (Bell 1981, Bell *et al.* 1984). Surface rupture from the July event occurred along a single structural segment, whereas surface rupture from the August event occurred along two structural segments and overlapped for about 12 km with the July surface ruptures.

1954 *Fairview Peak–Dixie Valley, Nevada, earthquakes*

The Fairview Peak and Dixie Valley earthquakes of 16 December 1954 (M_s7.2 and 6.8, respectively; Bonilla *et al.* 1984, Doser 1986) produced a complex pattern of surface ruptures in a 102 km by 32 km N-trending belt in west-central Nevada (Fig. 1). The Fairview Peak earthquake produced a 67-km-long N-trending zone of normal-right oblique-slip on three primary traces (Fig. 8): the Fairview Peak, Westgate and Gold King faults. the focal-plane solution of Doser (1986) has a preferred nodal plane that strikes N10°W, dips 60°NE, and has a significant right-lateral component. The Dixie Valley earthquake followed the Fairview Peak event by about 4½ min and caused dominantly normal-slip surface rupture along the eastern flank of the Stillwater Range (Fig. 9).

The northern end of surface faulting attributed to the Fairview Peak earthquake is near a small salient in Louderback Mountain and where the Dixie Valley widens considerably (Fig. 8, point D). The southern end of surface faulting splits into multiple discontinuous ruptures south of Bell Flat, and extends south of Mount Anna.

Three structural segments are interpreted for the Fairview Peak event based on surface rupture along three different faults, the Fairview, Gold King and Westgate faults. The Fairview segment ruptured approximately 32 km along the eastern base of Slate Mountain, Fairview Peak, and Chalk Mountain. Normal-right oblique-slip dominated, with maximum displacements of 3.7 m right-lateral, and 3.1 m normal-slip (Slemmons 1957). The Fairview segment rupture

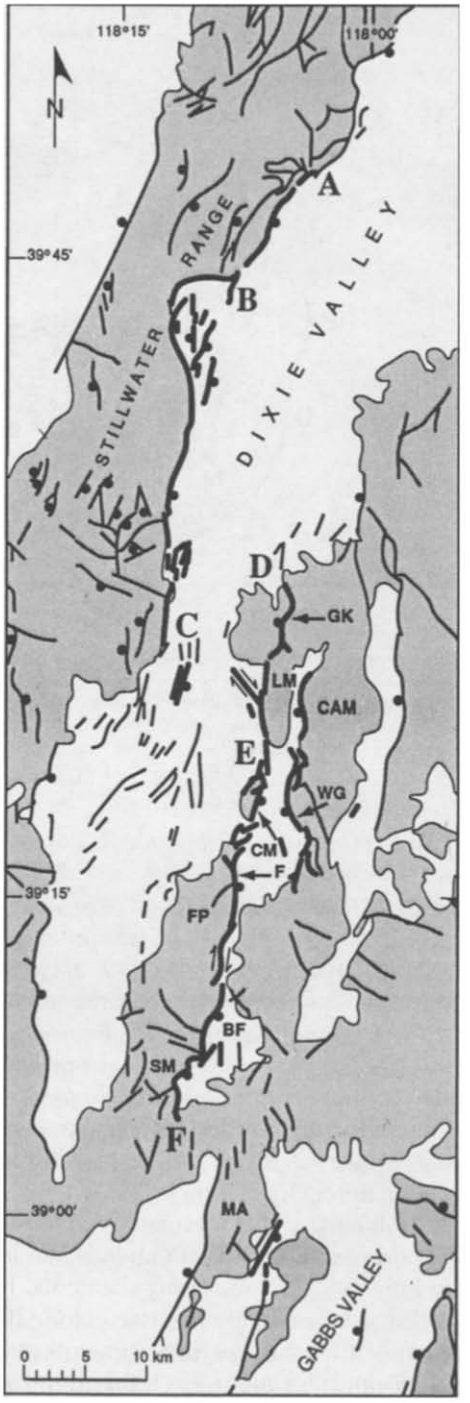

Fig. 8. Surface ruptures from the 1954 Fairview Peak and Dixie Valley earthquakes (from Slemmons 1957, Bell 1984, P. Zhang, personal communication 1990). GK = Gold King segment, LM = Louderback Mountain, CAM = Clan Alpine Mountains, WG = West Gate segment, CM = Chalk Mountain, MA = Mount Anna. Bedrock from Page (1965), Willden & Speed (1974) and Stewart & Carlson (1978). Annotation as Fig. 2.

follows the Fairview Peak range front north to where it branches into a series of NE-trending en échelon breaks, then continues as a range-front fault along Chalk Mountain and across an alluviated gap south of Louderback Mountain (Fig. 8, point E). Surface rupture continued for a distance of ~16 km to the north on the W-dipping Gold King segment, partly along the western edge of Louderback Mountain and partly in bedrock

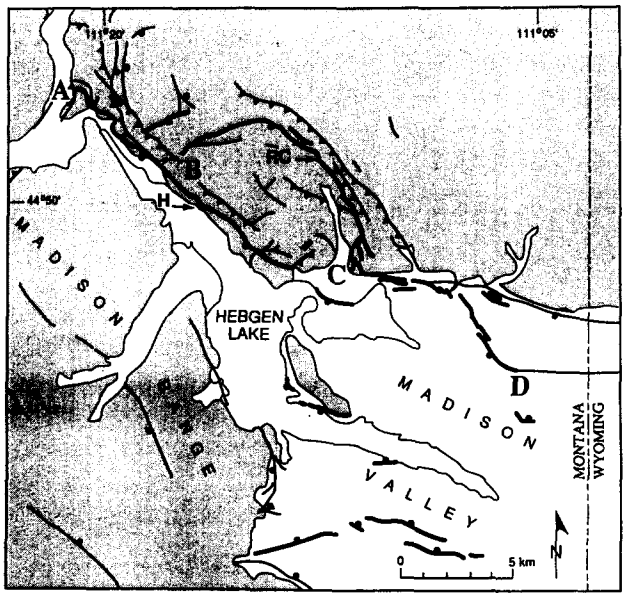

Fig. 9. Surface ruptures from the 1959 Hebgen Lake earthquake (surface ruptures and bedrock from U.S. Geological Survey 1964). H = Hebgen segment, RC = Red Canyon segment. Red Canyon is the alluvial valley just north of point C. Annotation as Fig. 2.

within the range. The Fairview and Gold King segments can be distinguished both structurally, because they occurred on faults that bound opposite sides of mountain blocks and have opposite dips, and behaviorally, based on differences in the amount of lateral slip and downthrown sides. Normal-slip displacements on the Gold King segment of as much as 60 cm may have been similar to surface displacement on this segment during the 1903(?) Wonder earthquake (Slemmons *et al.* 1959). This is one of the few cases of recurrent historical surface faulting in the United States. Recent field work indicates a significant component of right-lateral slip along a fault trace that splays away from the Gold King segment, northwestward into Dixie Valley (P. Zhang, personal communication 1990). The Westgate segment is a west-side-down range-front fault that parallels and is 2–4 km east of the Fairview and Gold King segments. Eighteen kilometers of surface rupture occurred along the Westgate segment, with maximum displacements of approximately 1 m normal slip and 0.5 m right-lateral slip.

Waveform inversion modeling by Doser (1986) indicates that the Fairview Peak event was a double and possibly triple event. However, this can not be clearly related to the segmentation model presented here. It is unclear how the seismic moment was distributed between these segments and how much of this faulting was secondary or sympathetic. For example, the Westgate and Gold King segments may be secondary or sympathetic ruptures in relation to the primary rupture of the Fairview segment.

The Dixie Valley earthquake ruptured a zone 43–47 km long on the west side of Dixie Valley. Rupture during this event probably did not cross a 10-km-wide left-step across Dixie Valley to the Fairview Peak rupture, although the distinctions of surface faulting produced by the two closely spaced earthquakes is conjectural. Normal displacements of more than 2 m were measured along the Dixie Valley rupture (Slemmons 1957). The southern end of surface faulting coincides approximately with the southeastern end of the Stillwater Range, and had a complex, distributed rupture pattern (Fig. 8, point C).

The Dixie Valley earthquake ruptured through a large range-front re-entrant, called "the bend", and surface faulting continued for about 12 km north of a ~40° change in the strike of the range-front fault (Fig. 8, point B). The portion of the fault north of the bend is considered a second geometric segment based on these changes. Displacement along this segment was generally about 0.5 m or less. The northern end of the surface rupture (Fig. 8, point A) coincides with a 0.8 km right step in the fault zone and a cross fault in the range (P. Zhang personal communication 1989). This cross fault may be part of a N-trending fault zone within the Stillwater Range that intersects, and may disrupt, a NE-trending fault pattern to the southwest. A magnetic anomaly associated with the Humboldt lopolith crosses the Dixie Valley fault in the general vicinity of the northern end of the 1954 rupture. Speed (1976) estimated the thickness (depth) of the lopolith as just over 1 km from the surface, using gravity and geologic data. Such a shallow feature in the crust probably would not have affected the rupture at depth, but may have influenced the near-surface rupture pattern.

The range front and late Quaternary fault scarps are essentially continuous beyond the northern limit of the Dixie Valley rupture. Bell & Katzer (1990) postulated that the northern part of the Dixie Valley earthquake rupture overlapped with the adjacent earthquake segment to the north, possibly by as much as 25 km. This is an important example of how significant overlap of earthquake segments can occur, and can potentially be identified.

In summary, surface faulting during the 1954 Fairview Peak–Dixie Valley earthquakes occurred mainly at or near the alluvium–bedrock range-front boundary and nearly always followed prehistoric fault scarps (Slemmonds 1957). At least three complex structural segments failed during the Fairview Peak earthquake: the Fairview segment, the Gold King segment and the Westgate segment. The Dixie Valley earthquake appears to have ruptured two geometric segments along the Dixie Valley fault zone.

1959 *Hebgen Lake, Montana, earthquake*

The 18 August 1959 Hebgen Lake earthquake (M_s7.5) (Doser 1985) produced a complex, 28-km-long (end-to-end distance, including secondary, antithetic ruptures), surface-rupture pattern near the southern end of the Madison Range in southwestern Montana. The event was felt over 870,000 km^2 (Stover 1985) and produced dramatic fault scarps, landslides and large-scale basin subsidence. The main shock is the largest earthquake recorded in the Intermountain seismic belt. Seismologic data suggest that the event was composed

of two principal subevents about 5 s apart on one or more WNW-trending fault planes dipping 45–60°S, with pure dip-slip motion (Doser 1985).

Pronounced normal-slip displacement occurred on the Red Canyon and Hebgen faults (structural segments) (Fig. 9), with secondary and minor displacement on several additional faults. The Red Canyon and Hebgen faults strike chiefly W to NW, discordant to the NNW trend of the prominent Madison Range. The Red Canyon fault ruptured for 23 km in a complex, curving trace that closely paralleled Laramide-age (late Cretaceous to early Cenozoic) fold axes and thrust fault surfaces (Witkind *et al.* 1962). The maximum vertical displacement (D_{max} = 4.6 m) occurred where bedding and pre-existing fault planes were favorably oriented for S- to SW-dipping normal slip (Myers & Hamilton 1964). The 12-km-long Hebgen fault rupture (D_{max} = 5.5 m) similarly appears to have been controlled by Laramide structures (Witkind *et al.* 1962). The end-to-end length of the ruptures along the Hebgen and Red Canyon faults is about 24 km.

Several faults antithetic to the Hebgen and Red Canyon faults also ruptured during this event, forming a large graben which was downdropped at the time of the earthquake (Myers & Hamilton 1964). These breaks were generally along small faults and monoclines, and are secondary in origin. There was also a 2.4-km-long sympathetic surface rupture along the west side of the Madison Range (not shown in Fig. 9). These breaks were about 11 km from the nearest primary surface rupture (Hebgen fault) and had as much as 1 m of vertical offset (Myers & Hamilton 1964).

At least two discrete structural segments failed during the 1959 Hebgen Lake earthquake, the Red Canyon and Hebgen faults. The Red Canyon rupture can be subdivided into two smaller geometric segments. At the mount of Red Canyon, the Red Canyon rupture had a pronounced change in scarp continuity, height and complexity. At this point (Fig. 9, point C), the rupture splayed into numerous traces, made a bend of about 60°, and occupied the same geomorphic position as the Hebgen fault, potentially merging with the Hebgen fault at depth. The southeastern end of the rupture is at a 55° bend in the fault zone within alluvium in Madison Valley (Fig. 9, point D). The northwestern end of the Hebgen fault rupture is at a cross fault (Fig. 9, point A). The Red Canyon and Hebgen fault segments could have been delineated on the basis of pre-existing fault scarps along much of their lengths, depite their relatively subdued geomorphic expression and the Red Canyon fault's location within the range (Witkind *et al.* 1962, Hall & Sablock 1985).

1983 *Borah Peak, Idaho, earthquake*

The M_s7.3 Borah Peak earthquake of 28 October 1983 produced about 36 km of surface rupture at the western base of the Lost River Range in east-central Idaho (Crone & Machette 1984). The event was felt over 670,000 km^2 of the United States and a large part of

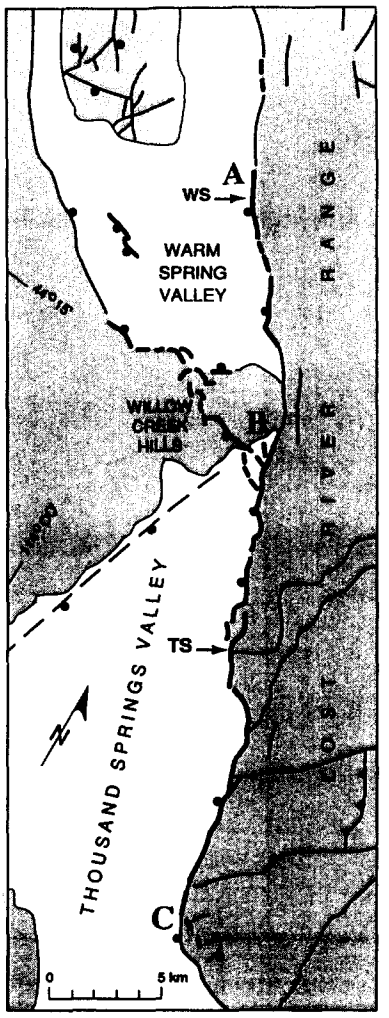

Fig. 10. Surface ruptures from the 1983 Borah Peak earthquake (from Crone & Machette 1984, Susong *et al.* 1990). Bedrock from Bond (1978) and Rember & Bennett (1979a, b). WS = Warm Springs segment, TS = Thousand Springs segment. Annotation as Fig. 2.

western Canada (Stover 1985). It produced surface faulting on two well-defined segments of the 140-km-long Lost River fault and a branch fault (Scott *et al.* 1985). Doser & Smith's (1985) preferred fault-plane solution of N48°W, 45°W, with approximately 5:1 normal to left-lateral displacement, agrees closely with measurements of surface slip. Rupture is believed to have propagated unilaterally to the northwest from a nucleation point 15–16 km deep near the southern end of surface faulting (Doser & Smith 1985).

Surface rupture (Fig. 10) occurred on three main traces: from south to north, a 21-km-long section of the Lost River fault that constitutes the main rupture and includes the maximum vertical displacement of 2.7 m and a maximum left-lateral offset of 0.7 m; a 14-km-long WNW-trending branching rupture across a series of bedrock hills (Willow Creek Hills) and out onto Antelope Flat (D_{max} = 1.6 m); and a 8-km-long northern rupture (D_{max} = 1 m) that also coincides with the Lost River fault (Crone & Machette 1984, Crone *et al.* 1987). The Lost River fault has been divided into six or seven discrete fault segments based on differing geomorphic expression, structural relief and ages of most recent

surface faulting (Scott *et al.* 1985). The southern and northern sections of the 1983 ruptures correspond to the Thousand Springs segment and the central portion of the Warm Spring segment of the Lost River fault, respectively. A gap in surface faulting at Willow Creek Hills separates these two segments (Fig. 10, point B); these two segments are considered geometric segments based on this gap in surface faulting.

The southern end of the Thousand Springs segment is marked by transverse faults in bedrock and an abrupt change in the strike of the range-front forming a salient (Fig. 10, point C). Susong *et al.* (1990) mapped NE- and NW-trending sets of faults within the bedrock; some of the NW-trending faults had minor surface displacement in 1983 (Vincent & Bull 1989). Susong *et al.* (1990) suggested that these networks of faults mark the nucleation point of the rupture and acted to arrest the spread of the rupture to the south. The rupture appears to have propagated northwestward from near this point some 20 km along the Lost River fault to a transverse bedrock ridge (Willow Creek Hills) between Thousand Springs and Warm Spring Valleys (Fig. 10, point B), where it was partially deflected west-northwest (Crone *et al.* 1985). Faulting on the range front continued for about 8 km to the northwest on the Warm Spring segment, after a gap of 4.8 km, and died out along the range-front fault (Fig. 10, point A) (Crone & Machette 1984). Surface cracks with little or no displacement are locally present for another 5 km to the north (Crone *et al.* 1985). If these cracks are included, the total length would increase to >39 km.

Crone & Haller (1991) point out that although the total length of surface faulting is 36 km, most of the seismic moment release from the main shock was associated with rupture of the Thousands Springs segment, and that surface rupture along the Warm Spring segment is secondary or sympathetic in nature. The boundary between these two segments is described as "leaky" by Crone & Haller, essentially terminating the rupture, but allowing minor displacement at depth and/or strong ground motion to trigger slip on the Warm Spring segment. Likewise, the branching rupture through Willow Creek Hills is thought to be secondary. Because of the branching structural discontinuity, this is considered a separate structural segment.

The style and amount of displacement in 1983 was similar to a mid-Holocene (Hanks & Schwartz 1987, Cluer 1988) event documented on the Thousand Springs segment (Hait & Scott 1978, Schwartz & Crone 1985). Similarities between the two most recent events on this segment support the earthquake segmentation and characteristic earthquake model (Schwartz & Coppersmith 1984). The most recent paleoseismic event along the Warm Spring segment occurred just prior to 5.5–6.2 ka (Schwartz & Crone 1988), about the same time as the mid-Holocene event on the Thousand Springs segment. However, surface displacements along the Warm Spring segment from this paleoearthquake were at least twice as much as those from the 1983 event, and surface ruptures were much more extensive (D. P. Schwartz personal communication 1988). A single mid-Holocene event may have ruptured both the Thousand Springs and Warm Spring segments, but with larger displacements along the Warm Spring segment than occurred in 1983. Alternatively, a second earthquake may have occurred along the Warm Spring segment relatively close in time to the mid-Holocene event on the Thousand Springs segment or following a prior "1983-type" event (D. P. Schwartz personal communication 1988).

Table 2. Summary of segmentation of historical Basin and Range province surface-faulting events. Number of fault segments interpreted in this study and types of discontinuities represented are listed. G = geometric discontinuity, S = structural discontinuity, B = behavioral discontinuity

Date/Event	Magnitude	Fault segments
1872 Owens Valley	7.7–8+	3 G, B
1887 Sonora	7.2–7.4	2–3 G
1915 Pleasant Valley	7.6	4–5 G, S
1932 Cedar Mountain	7.2	>3 G, S
1950 Fort Sage	5.6	1 G
1954 Rainbow Mountain	6.3	1 S
1954 Stillwater	7	2 S
1954 Fairview Peak	7.2	3–4+ S, B
1954 Dixie Valley	6.8	2 G
1959 Hebgen Lake	7.5	2–3 G, S
1983 Borah Peak	7.3	2–3 S

DISCUSSION

The 11 historical events associated with surface faulting in the Basin and Range province exhibit a large degree of variability in the amount and style of surface rupture. Some surface ruptures are concentrated along range fronts in relatively narrow zones (e.g. 1954 Dixie Valley and 1983 Borah Peak earthquakes), whereas other ruptures are complex and widely distributed (e.g. 1932 Cedar Mountain and 1954 Fairview Peak earthquakes). Moderate and strong earthquakes (magnitude 5–7) tended to cause simpler surface ruptures than the larger events. The eight earthquakes with magnitude ≥7 ruptured multiple geometric or structural segments (Table 2); these include the 1872 Owens Valley earthquake (three geometric segments) and the 1915 Pleasant Valley earthquake (four or five structural or geometric segments). Failure of these multiple segments may be responsible for some of the multiple ruptures observed by seismologists for large events in the Basin and Range province (Doser & Smith 1989, Jackson & White 1989).

Many of the largest events (magnitude ≥7.2) involved complex, widely distributed rupture patterns (e.g. 1915 Pleasant Valley, 1932 Cedar Mountain and 1954 Fairview Peak earthquakes). These events ruptured consecutive and parallel structural segments along range fronts and across ranges and valleys and produced complicated patterns of surface faulting involving primary, secondary and sympathetic displacements. Some possible underlying causes for the complex and widely distributed surface ruptures in the Basin and Range province include: (1) decoupling and detachment faulting in

the mid to upper crust (Burchfiel 1965, Hardyman 1978, 1984, Wallace 1979, 1989, Molinari 1984a); (2) occurrence in heterogeneous, highly tectonized crust with pre-existing structures and fabrics, and varying lithologies; (3) triggering of multiple ruptures either by exceedence of seismic failure thresholds of adjacent faults or through sympathetic displacement; and (4) significant or dominant strike-slip displacement components that cut across pre-existing structural grains or splay upwards (flower structures).

Additional detailed paleoseismic studies will be important for determining to what extent the complex patterns of historical ruptures are the result of characteristic earthquakes that ruptured similar multiple geometric and structural segments during past events (Schwartz & Coppersmith 1984, 1986, Schwartz 1988). In cases where paleoearthquakes are clustered spatially and temporally, it may be difficult to delineate individual earthquake segments from paleoseismic data alone. For example, at some future time, using only paleoseismic techniques, it would be difficult to distinguish between the 1954 Rainbow Mountain and Stillwater earthquakes, or to temporally differentiate the historical ruptures in the Central Nevada seismic belt.

Approximately half of the 11 historical surface ruptures ended at discontinuities that could have been identified as indicators of fault-zone discontinuities based on such characteristics as cross faults, branch faults, extensional basins, ends of mountain ranges, transverse-bedrock ridges and salients. The other half were either widely distributed with indistinct end points, or ended at locations at the surface that did not coincide with clear indicators of fault zone discontinuities.

The structural and geometric segment lengths from these earthquakes fall in three groupings: (1) 8.5–12 km; (2) 17–23 km; and (3) 30–39 km. The middle grouping clusters near a proposed general maximum segment length of 20 km for normal faults (Jackson & White 1989). However, two of the segments considered here from dominantly normal-slip displacement earthquakes had significantly longer lengths: the 1887 Sonora earthquake (central segment—39+ km) and the 1915 Pleasant Valley earthquake (Pearce segment—30 km).

Recent studies of well-recorded historical events have concluded that seismic moment release may be concentrated along portions of a fault or earthquake segment, or dominated by an individual segment (e.g. 1983 Borah Peak earthquake). Unfortunately, with the exception of the 1983 Borah Peak earthquake, it is difficult to clearly discern which segments may have dominated the moment release, although some speculations can be made based on multiple-event interpretations from analysis of seismgrams, variations in the amount of surface rupture, and fault geometry relative to the main rupture.

As is the case for most of the 11 events, the magnitude of the 1983 Borah Peak earthquake (M_s7.3) was considerably larger than what would be estimated for individual segments of the Lost River fault zone (Freeman *et al.* 1986). Rupture of the 22-km-long Thousand Springs segment alone yields an estimated magnitude M_s6.7–6.8 event, using magnitude vs fault-length relations from Slemmons (1982) and Bonilla *et al.* (1984). A 36 km rupture length yields an estimated magnitude of M_s6.9–7.1. This underscores the importance of considering uncertainties in estimated magnitudes, as well as potential multiple segment failures. Further, the use of other fault parameters, such as maximum surface displacement, for determining magnitude values can help cross-check individual estimates of earthquake size.

CONCLUSIONS

Surface ruptures from historical earthquakes in the Basin and Range province have exhibited a wide variety of faulting patterns, from simple to complex. Moderate and strong earthquakes have tended to cause simpler surface ruptures, whereas, surface ruptures from events of magnitude 7 and greater have involved the failure of multiple geometric or structural segments. Many of the events larger than magnitude 7.2 had complex, widespread surface-rupture patterns.

Approximately half of the endpoints of historical Basin and Range province surface ruptures coincided with distinct fault-zone discontinuities. The other half ended in either widely distributed breaks and/or did not coincide with clear indicators of discontinuities. In several cases, historical surface faulting has ruptured through or occurred on both sides of pronounced geometric and structural discontinuities. Thus, some earthquake discontinuities may be difficult to identify and significant faulting may occur beyond postulated discontinuities. Several lines of evidence are required to evaluate earthquake discontinuities, one of the most important of which is timing information for past earthquakes.

These observations indicate that simple earthquake segmentation models may be inadequate for evaluating larger earthquakes in the Basin and Range province. Seismic hazard assessments in the province should consider ruptures of multiple geometric or structural segments, and should rely on different types of data and large uncertainties in earthquake segment lengths and earthquake-size estimations. Further studies of historical earthquakes and fault zone behavior, and the development of new information, such as geophysical and paleoseismic data, will increase our understanding of the complexities of earthquake ruptures in extensional provinces. With additional data, behavioral models can be developed for fault zones (e.g. Machette *et al.* 1989) and a more accurate understanding and delineation of earthquake segments may be possible.

Acknowledgements—We would like to thank Sarah Beanland, John Bell, Diane dePolo, Dick Meeuwig, Phil Pearthree and, especially, Tony Crone for useful discussions, comments and reviews which improved the manuscript. Special thanks also to Kris Pizarro of the Nevada Bureau of Mines and Geology for preparing the figures. This study was supported in part by a grant from the Nevada Nuclear Waste Project Office.

REFERENCES

Abe, K. 1981. Magnitudes of large shallow earthquakes from 1904 to 1980. *Phys. Earth. & Planet. Interiors* **27**, 72–80.

Albee, A. L. & Smith, J. L. 1966. Earthquake characteristics and fault activity in southern California. In: *Engineering Geology in Southern California* (edited by Lung, R. & Proctor, R.). Ass. Engng Geol., Los Angeles Section, 9–34.

Barka, A. A. & Kadinsky-Cade, K. 1988. Strike-slip fault geometry in Turkey and its influence on earthquake activity. *Tectonics* **7**, 663–684.

Beanland, S. & Clark, M. 1987. The Owens Valley fault zone, and surface rupture associated with the 1872 earthquake (Abs.). *Seism. Res. Lett.* **58**, 32.

Beanland, S. & Clark, M. C. In press, The Owens Valley fault zone, eastern California, and surface rupture associated with the 1872 earthquake. *Bull. U.S. geol. Surv.*

Bell, J. W. 1981. Quaternary fault map of the Reno 1° by 2° quadrangle. *U.S. geol. Surv. Open-file Rep.* **81–982**.

Bell, J. W. 1984. Quaternary fault map of Nevada–Reno sheet. 1/250,000 scale map. *Nevada Bur. Mines & Geol. Map* 79.

Bell, J. W. & Katzer, T. 1990. Timing of late Quaternary faulting in the 1954 Dixie Valley earthquake area, central Nevada. *Geology* **18**, 622–625.

Bell, J. W., Slemmons, D. B. & Wallace, R. E. 1984. Roadlog: Reno to Dixie Valley–Fairview Peak earthquake areas. In: 1984 *Geol. Soc. Am. Ann. Meet., West. Geol. Excurs. Guidebook* 4 (edited by Lintz, J.), 425–472.

Bond, J. G. 1978. Geologic map of Idaho. 1/500,000 scale map. Idaho Bur. Mines & Geol.

Bonham, H. F. 1969. Geology and mineral deposits of Washoe and Storey Counties, Nevada. *Bull. Nevada Bur. Mines & Geol.* **70**.

Bonilla, M. G.. Mark, R. K. & Lienkaemper, J. J. 1984. Statistical relations among earthquake magnitude, surface rupture length, and surface fault displacement. *Bull. seism. Soc. Am.* **74**, 2379–2411.

Bull, W. B. & Pearthree, P. A. 1988. Frequency and size of Quaternary surface ruptures of the Pitaycachi fault, northeastern Sonora, Mexico. *Bull. seism. Soc. Am.* **78**, 956–978.

Burchfiel, B. C. 1965. Structural geology of the Specter Range quadrangle, Nevada, and its regional significance. *Bull. geol. Soc. Am.* **76**, 175–192.

Burnett, J. L. & Jennings, C. W. 1962. Geologic map of California, Chico Sheet. 1/250,000 scale map. Calif. Div. Mines & Geol.

Carver, G. A. 1969. Quaternary tectonism and surface faulting in the Owens Lake Basin, California. Unpublished M.S. thesis, University of Nevada, Reno.

Cluer, J. K. 1988. Quaternary geology of Willow Creek and some age constraints on prehistoric faulting, Lost River Range, east-central Idaho. *Bull. seism. Soc. Am.* **78**, 946–955.

Coffman, J. L. & von Hake, C. A. 1973. Earthquake history of the United States, revised edition (through 1970). *U.S. Dept Commerce Publ.* **41–1**.

Crone, A. J. & Haller, K. M. 1991. Segmentation and the coseismic behavior of Basin and Range normal faults: examples from east-central Idaho and southwestern Montana, U.S.A. *J. Struct. Geol.* **13**, 151–164.

Crone, A. J. & Machette, M. N. 1984. Surface faulting associated with the Borah Peak earthquake, central Idaho. *Geology* **12**, 664–667.

Crone, A. J., Machette, M. N., Bonilla, M. G., Lienkaemper, J. J., Pierce, K. L., Scott, W. E. & Bucknam, R. C. 1985. Characteristics of surface faulting accompanying the Borah Peak earthquake, central Idaho. *U.S. geol. Surv. Open-file Rep.* **85–290**, 43–58.

Crone, A. J., Machette, M. N., Bonilla, M. G., Leinkaemper, J. J., Pierce, K. L., Scott, W. E. & Bucknam, R. C. 1987. Surface faulting accompanying the Borah Peak earthquake and segmentation of the Lost River fault, central Idaho. *Bull. seism. Soc. Am.* **77**, 739–770.

dePolo, C. M., Bell, J. W. & Ramelli, A. R. 1987a. Geometry of strike-slip faulting related to the 1932 Cedar Mountain earthquake, central Nevada. *Geol. Soc. Am. Abs. w. Prog.* **19**, 371.

dePolo, C. M., Clark, D. G., Slemmons, D. B. & Aymard, W. H. 1989. Historical Basin and Range province surface faulting and fault segmentation. *U.S. geol. Surv. Open-file Rep.* **89–315**, 131–163.

dePolo, C. M., Ramelli, A. R. & Bell, J. W. 1987b. Visit to trenches along the southern part of the 1932 Cedar Mountain earthquake ruptures, Monte Cristo Valley, Nevada. Unpublished field guide, Nevada Bur. Mines & Geol.

dePolo, C. M. & Slemmons, D. B. In press. Estimation of earthquake size for seismic hazards. *Geol. Soc. Am. Rev. Engng. Geol.* **3**.

Direccion General de Geografia del Territorio Nacional. 1981. Carta Geologica, Tijuana Sheet. 1/1,000,000 scale map. Secretaria de Programacion y Presupuesto, Estados Unidos Mexicanos.

Doser, D. I. 1985. Source parameters and faulting processes of the 1959 Hebgen Lake, Montana, earthquake sequence. *J. geophys. Res.* **90**, 4537–4555.

Doser, D. I. 1986. Earthquake processes in the Rainbow Mountain–Fairview Peak–Dixie Valley, Nevada, region 1954–1959. *J. geophys. Res.* **91**, 12,572–12,586.

Doser, D. I. 1988. Source parameters of earthquakes in the Nevada seismic zone, 1915–1943. *J. geophys. Res.* **93**, 15,001–15,015.

Doser, D. I. & Smith, R. B. 1985. Source parameters of the 28 October 1983 Borah Peak, Idaho, earthquake from body wave analysis. *Bull. seism. Soc. Am.* **75**, 1041–1051.

Doser, D. I. & Smith, R. B. 1989. An assessment of source parameters of earthquakes in the Cordillera of the Western United States. *Bull. seism. Soc. Am.* **79**, 1383–1409.

Dubois, S. M. & Sbar, M. L. 1981. The 1887 earthquake in Sonora: Analysis of regional ground shaking and ground failure. *U.S. geol. Surv. Open-file Rep.* **81–437**.

Dubois, S. M. & Smith, A. W. 1980. The 1887 earthquake in San Bernardino Valley, Sonora: Historical accounts and intensity patterns in Arizona. *Spec. Tech. Pap. Arizona Bur. Geol. & Min.* **3**.

Dunne, G. C., Rachel, M. G. & Sylvester, A. G. 1978. Mesozoic evolution of rocks of the White, Inyo, Argus and Slate Ranges, eastern California. In: *Mesozoic Paleogeography of the Western United States, Pacific Coast Paleogeography Symposium* 2. *Soc. econ. Paleont. Miner.*, 189–207.

Fonseca, J. 1988. The Sou Hills: a barrier to faulting in the central Nevada seismic belt. *J. geophys. Res.* **93**, 475–489.

Freeman, K. J., Fuller, S. & Schell, B. A. 1986. The use of surface faults for estimating design earthquakes; implications of the 28 October 1983, Idaho earthquake. *Ass. Engng. Geol.* **23**, 325–332.

Gianella, V. P. 1951. Fort Sage Mountain, California, earthquake of December 14, 1950. *Bull. geol. Soc. Am.* **62**, 1502.

Gianella, V. P. 1957. Earthquake and faulting, Fort Sage Mountains, California, December, 1950. *Bull. seism. Soc. Am.* **47**, 173–177.

Gianella, V. P. & Callaghan, E. The Cedar Mountain, Nevada, earthquake of December 20, 1932. *Bull. seism. Soc. Am.* **24**, 345–377.

Goodfellow, G. E. 1888. The Sonora earthquake. *Science* **11**, 162–166.

Grose, T. L. T. 1984. Geologic map of the State Line Peak Quadrangle, Nevada–California. *Nevada Bur. Mines Geol. Map* 82.

Hait, M. H., Jr. & Scott, W. E. 1978. Holocene faulting, Lost River Range, Idaho. *Geol. Soc. Am. Abs. w. Prog.* **10**, 217.

Hall, W. B. & Sablock, P. E.. 1985. Comparison of the geomorphic and surficial fracturing effects of the 1983 Borah Peak, Idaho earthquake with those of the 1959 Hebgen Lake, Montana earthquake. *U.S. geol. Surv. Open-file Rep.* **85–290**, 141–152.

Hanks, T. C. & Kanamori, H. 1979. A moment magnitude scale. *J. geophys. Res.* **84**, 2348–2350.

Hanks, T. C. & Schwartz, D. P. 1987. Morphologic dating of the pre-1983 fault scarp on the Lost River fault at Doublespring Pass Road, Custer County, Idaho. *Bull. seism. Soc. Am.* **77**, 837–846.

Hardyman, R. F. 1978. Volcanic stratigraphy and structural geology of the Gillis Canyon quadrangle, northern Gillis Range, Mineral County, Nevada. Unpublished Ph.D. thesis, University of Nevada, Reno.

Hardyman, R. F. 1984. Strike-slip, normal, and detachment faults in the northern Gillis Range, Walker Lane of west central Nevada. In: 1984 *Geol. Soc. Am. Ann. Meet., West. Geol. Excurs. Guidebook* 4 (edited by Lintz, J.), 184–199.

Herd, D. G. & McMasters, C. R. 1982. Surface faulting in the Sonora, Mexico, earthquake of 1887. *Geol. Soc. Am. Abs. w. Prog.* **14**, 172.

Jackson, J. A. & White, N. J. 1989. Normal faults in the upper continental crust: observations from regions of active extension. *J. Struct. Geol.* **11**, 15–36.

Kanamori, H. 1983. Magnitude scale and quantification of earthquakes. *Tectonophysics* **93**, 185–199.

Knuepfer, P. L. K. 1989. Implications of the characteristics of end-points of historical surface fault ruptures for the nature of fault segmentation. *U.S. geol. Surv. Open-file Rep.* **89–315**, 193–228.

Knuepfer, P. L. K., Bamberger, M. J., Turko, J. M. & Coppersmith, K. J. 1987. Characteristics of the boundaries of historical surface fault ruptures. *Seism. Res. Lett.* **58**, 31.

Lebetkin, L. K. C. & Clark, M. C. 1988. Late Quaternary activity along the Lone Pine fault, eastern California. *Bull. geol. Soc. Am.* **100**, 755–766.

Lydon, P. A., Gay, T. E., Jr. & Jennings, C. W. 1960. Geologic map of California, Westwood Sheet. *Calif. Div. Mines & Geol.*

Machette, M. N., Personius, S. F., Nelson, A. R., Schwartz, D. P. & Lund, W. R. 1989. Segmentation models and Holocene movement history of the Wasatch fault zone, Utah. *U.S. geol. Surv. Open-file Rep.* **89–315**, 229–245.

Martel, S. J. 1984. Structure of the Owens Valley fault zone near Poverty Hills, Owens Valley, California. *Geol. Soc. Am. Abs. w. Prog.* **16**, 585.

Matthews, R. A. & Burnett, J. L. 1965. Geologic map of California, Fresno Sheet. 1/250,000 scale map. *Calif. Div. Mines & Geol.*

Molinari, M. P. 1984a. Late Cenozoic geology and tectonics of Stewart and Monte Cristo Valleys, west-central Nevada. Unpublished M.S. thesis, University of Nevada, Reno.

Molinari, M. P. 1984b. Late Cenozoic structural geology of Stewart and Monte Cristo Valleys, Walker Lane of west-central Nevada. In: 1984 *Geol. Soc. Am. Ann. Meet., West. Geol. Excurs. Guidebook* 4 (edited by Lintz, J.), 219–231.

Morrison, R. B. 1964. Lake Lahontan: Geology of southern Carson Desert, Nevada. *Prof. Pap. U.S. geol. Surv.* **401**.

Myers, W. B. & Hamilton, W. 1964. Deformation accompanying the Hebgen Lake earthquake of August 17, 1959. *Prof. Pap. U.S. geol. Surv.* **435-I**, 55–98.

Oakeshott, G. B., Greensfelder, R. W. & Kahle, J. E. 1972. 1872–1972 . . . one hundred years later. *Calif. Div. Mines. Geol. Calif. Geol.* **25**, 55–61.

Page, B. M. 1934. Basin-range faulting of 1915 in Pleasant Valley, Nevada. *J. Geol.* **43**, 690–707.

Page, B. M. 1965. Preliminary geologic map of a part of the Stillwater Range, Churchill County, Nevada. 1/125,000 scale map. *Nevada. Bur. Mines & Geol. Map* **28**.

Pearthree, P. A., Bull, W. B. & Wallace, T. C. 1990. Geomorphology and Quaternary geology of the Pitaycachi fault, northeastern Sonora, Mexico. *Spec. Pap. Arizona geol. Surv.* **7**, 124–135.

Rember, W. C. & Bennett, E. H. 1979a. Geologic map of the Challis quadrangle, Idaho. 1/250,000 scale map. *Idaho Bur. Mines & Geol.*

Rember, W. C. & Bennett, E. H. 1979b. Geologic map of the Dubois quadrangle, Idaho. 1/250,000 scale map. *Idaho Bur. Mines & Geol.*

Schwartz, D. P. 1988. Geologic characterization of seismic sources: moving into the 1990s. In: *Earthquake Engineering and Soil Dynamics II—Recent Advances in Ground Motion Evaluation* (edited by Von Thun, J. L.). *Geotech. Spec. Publs Am. Soc. Civil Engrs* **20**, 1–42.

Schwartz, D. P. & Coppersmith, K. J. 1984. Fault behavior and characteristic earthquakes: examples from the Wasatch and San Andreas fault zones. *J. geophys. Res.* **89**, 5681–5698.

Schwartz, D. P. & Coppersmith, K. J. 1986. Seismic hazards: New trends in analysis using geological data. In: *Active Tectonics, Studies in Geophysics* (edited by Wallace, R. E.). National Academy Press, Washington, DC, 215–230.

Schwartz, D. P. & Crone, A. J. 1985. The 1983 Borah Peak earthquake: a calibration event for quantifying earthquake recurrence and fault behavior on Great Basin normal faults. *U.S. geol. Surv. Open-file Rep.* **85–290**, 153–160.

Schwartz, D. P. & Crone, A. J. 1988. Paleoseismicity of the Lost River fault zone, Idaho: earthquake recurrence and segmentation. *Geol. Soc. Am. Abs. w. Prog.* **20**, 228.

Scott, W. E., Pierce, K. L. & Hait, M. H., Jr. 1985. Quaternary tectonic setting of the 1983 Borah Peak earthquake, central Idaho. *Bull. seism. Soc. Am.* **75**, 1053–1066.

Sibson, R. H. 1989. Earthquake faulting as a structural process. *J. Struct. Geol.* **11**, 1–14.

Slemmons, D. B. 1957. Geological effects of the Dixie Valley–Fairview Peak, Nevada, earthquakes of December 16, 1954. *Bull. seism. Soc. Am.* **47**, 353–375.

Slemmons, D. B. 1982. Determination of design earthquake magnitudes for microzonation. In: *Proc. 3rd Int. Earthquake Microzonation Conf.* (Seattle, Washington, June 28–July 1), Vol. 1, 119–130.

Slemmons, D. B. & dePolo, C. M. 1986. Evaluation of active faulting and associated hazards. In: *Active Tectonics, Studies in Geophysics* (edited by Wallace, R. E.). National Academy Press, Washington, DC, 45–62.

Slemmons, D. B., Steinbrugge, K. V., Tocher, D., Oakeshott, G. B. & Gianella, V. P. 1959. Wonder, Nevada, earthquake of 1903. *Bull. seism. Soc. Am.* **49**, 251–265.

Speed, R. C. 1976. Geologic Map of the Humboldt lopolith and surrounding terrane, Nevada. *Geol. Soc. Am. Map* **MC-14**.

Stewart, J. H. 1980. Regional tilt patterns of late Cenozoic basin-range fault blocks in the Great Basin. *Bull. geol. Soc. Am.* **91**, 460–464.

Stewart, J. H. 1983. Cenozoic structure and tectonics of the northern Basin and Range province, California, Nevada, and Utah. In: *The Role of Heat in the Development of Energy and Mineral Resources in the Northern Basin and Range province*. Geothermal Resources Council, 25–40.

Stewart, J. H. & Carlson, J. E. 1978. Geologic map of Nevada. 1/500,000 scale map. *U.S. geol. Surv. and Nevada Bur. Mines & Geol.*

Stover, C. W. 1985. Isoseismal map and intensity distribution for the Borah Peak, Idaho, earthquake of October 28, 1983. *U.S. geol. Surv. Open-file Rep.* **85–290**, 401–408.

Streitz, R, & Stinson, M. C. 1974. Geologic map of California, Death Valley Sheet. 1/250,000 scale map. *Calif. Div. Mines & Geol.*

Strand, R. G. 1967. Geological map of California, Mariposa Sheet. 1/250,000 scale map. *Calif. Div. Mines & Geol.*

Sumner, J. R. 1977. The Sonora earthquake of 1887. *Bull. seism. Soc. Am.* **67**, 1219–1223.

Susong, D. D., Janecke, S. V. & Bruhn, R. L. 1990. Structure of a fault segment boundary in the Lost River fault zone, Idaho, and possible effect on the 1983 Borah Peak earthquake rupture. *Bull. seism. Soc. Am.* **80**, 57–68.

Thenhaus, P. C. & Barnhard, T. P. 1989. Regional termination and segmentation of Quaternary fault belts in the Great Basin, Nevada and Utah. *Bull. seism. Soc. Am.* **79**, 1426–1438.

Tocher, D. 1956. Movement on the Rainbow Mountain fault. *Bull. seism. Soc. Am.* **46**, 10–14.

U.S. Geological Survey. 1964. The Hebgen Lake, Montana, earthquake of August 17, 1959. *Prof. Pap. U.S. geol. Surv.* **435**.

Vincent, K. R. & Bull, W. B. 1989. New Evidence of surface faulting from Borah peak earthquake and project summary. *U.S. geol. Surv. Summ. Tech. Reps.* **XXVIII**, 149–160.

Wallace, R. E. 1979. Earthquakes and the prefractured state of the western part of the North American continent. *Proc. Int. Res. Conf. Intra-Continental Earthquakes*, Ohrid, Yugoslavia.

Wallace, R. E. 1984a. Notes on surface faulting in Dixie Valley, Nevada. In: 1984 *Geol. Soc. Am. Ann. Meet., West. Geol. Excurs. Guidebook* 4 (edited by Lintz, J.), 402–407.

Wallace, R. E. 1984b. Fault scarps formed during the earthquakes of October 2, 1915, Pleasant Valley, Nevada and some tectonic implications. *Prof. Pap. U.S. geol. Surv.* **1274-A**.

Wallace, R. E. 1987. Grouping and migration of surface faulting and variations in slip rates on faults in the Great Basin province. *Bull. seism. Soc. Am.* **77**, 868–876.

Wallace, R. E. 1989. Fault-plane segmentation in brittle crust and anisotropy in loading system. *U.S. geol. Surv. Open-file Rep.* **89–315**, 400–408.

Wheeler, R. L. 1987. Boundaries between segments of normal faults: Criteria for recognition and interpretation. *U.S. geol. Surv. Open-file Rep.* **87–673**, 385–398.

Wheeler, R. L. & Krystinik, K. B. 1988. Segmentation of the Wasatch fault zone, Utah: Summaries, analyses, and interpretations of geological and geophysical data. *Bull. U.S. geol. Surv.* **1827**.

Willden, R. & Speed, R. C. 1974. Geology and mineral deposits of Churchill County, Nevada. *Bull. Nevada Bur. Mines & Geol.* **83**.

Witkind, I. J., Myers, W. B., Hadley, J. B., Hamilton, W. & Fraser, G. D. 1962. Geologic features of the earthquake at Hebgen Lake, Montana, August 17, 1959. *Bull. seism. Soc. Am.* **52**, 163–180.